

Circ_0061825 Acts as a miR-593-3p Sponge to Promote Breast Cancer Progression by Regulating FGFR3 Expression

This article was published in the following Dove Press journal:
Cancer Management and Research

Jiping Xie
Yi Wan
Min Zhang
Zeyu Jin
Yongqiang Yao

Third Ward of Breast and Thyroid Surgery
Department, Affiliated Zhongshan
Hospital of Dalian University, Dalian City,
Liaoning Province, People's Republic of
China

Background: Breast cancer (BC) remains the most common malignancy among women. Circular RNAs (circRNAs) have been demonstrated to play important roles in human cancers, including BC. In this study, we sought to identify the precise parts of circ_0061825 (circRNA trefoil factor 1, circ_TFF1) in BC pathogenesis.

Methods: The expression levels of circ_0061825, miR-593-3p and fibroblast growth factor receptor 3 (FGFR3) were detected by quantitative real-time polymerase chain reaction (qRT-PCR) or Western blot. Circ_0061825 was characterized using ribonuclease (RNase) R digestion, actinomycin D and subcellular fractionation assays. Cell viability, colony formation, migration, invasion, cell cycle progression and apoptosis were evaluated using Cell Counting Kit-8 (CCK-8), colony formation, wound-healing, transwell and flow cytometry assays, respectively. Targeted relationships among circ_0061825, miR-593-3p and FGFR3 were determined by a dual-luciferase reporter assay. Animal studies were used to assess the impact of circ_0061825 in tumor growth in vivo.

Results: Our data indicated that circ_0061825 was overexpressed in BC tissues and cells, and it was mainly localized in the cytoplasm of BC cells. Circ_0061825 knockdown hampered BC cell viability, colony formation, migration, invasion, cell cycle progression and enhanced cell apoptosis in vitro and weakened tumor growth in vivo. Mechanistically, circ_0061825 functioned as a molecular sponge of miR-593-3p, and circ_0061825 knockdown repressed BC cell malignant progression in vitro by miR-593-3p. FGFR3 was a direct target of miR-593-3p, and circ_0061825 modulated FGFR3 expression through sponging miR-593-3p. Moreover, miR-593-3p overexpression hindered BC cell malignant progression in vitro by down-regulating FGFR3.

Conclusion: Our current work provided evidence that circ_0061825, an up-regulated circRNA in BC, regulated BC malignant progression at least in part through targeting the miR-593-3p/FGFR3 axis, illuminating a novel therapeutic target for BC management.

Keywords: breast cancer (BC), circ_0061825, miR-593-3p, FGFR3

Introduction

Among women, breast cancer (BC) remains the most prevalent malignancy and the leading cause of cancer death worldwide in 2018.¹ Despite decades of research, our understanding for BC pathogenesis is still limited. Currently, the advancements in diagnosis and therapy have shown great benefits in declining BC recurrence and mortality.² Nevertheless, the overall survival of metastatic patients remains very low.³ Understanding the actions of the regulatory molecules in BC pathogenesis can provide a unique opportunity to design better therapeutic strategies.

Correspondence: Yongqiang Yao
Third Ward of Breast and Thyroid Surgery
Department, Affiliated Zhongshan Hospital
of Dalian University, No. 6 Jiefang Street,
Zhongshan District, Dalian 215004,
Liaoning Province, People's Republic of
China
Tel/Fax +86 0411-62897391
Email yyq760225@163.com

Circular RNAs (circRNAs), formed by back-splicing of pre-mRNA transcripts, are noncoding RNA molecules that play important roles from normal development to disease.⁴ Recent work has showed that hundreds of cytoplasmic circRNAs can weaken microRNA (miRNA) function through serving as miRNA sponges in cancers, including BC.^{5,6} For instance, Wang et al uncovered that circ_000911, a low expressed circRNA in BC, regulated BC cell malignant behaviors via sponging miR-449a.⁷ Zhang et al identified that circ_0052112 functioned as a potential promoter in BC metastasis via sequestering miR-125a-5p.⁸ Liu et al uncovered that circ_0008039 served as a miR-432-5p sponge to contribute to BC tumorigenesis via affecting the transcriptional activity of E2F transcription factor 3.⁹ Of interest, a recent report demonstrated that circ_0061825 (circRNA trefoil factor 1, circ_TFF1) was remarkably overexpressed in BC and the inhibition of circ_0061825 might serve as a therapeutic agent for BC management.¹⁰ Here, we sought to identify the biological role of circ_0061825 in BC pathogenesis.

Cancer in particular has been a major focus of miRNA research, and many studies have identified the pivotal involvement of miRNAs in BC pathophysiology.^{11,12} MiR-593-3p, a tumor-related miRNA,^{13,14} was uncovered to be underexpressed in BC cell lines.¹⁵ The findings by Song et al also demonstrated that miR-593-3p in BC cells was a molecular mediator of circ_0007534 in regulating BC cell malignant progression. Nevertheless, whether miR-593-3p is involved in the molecular basis of circ_0061825 in BC pathogenesis is not yet explored.

In this report, we undertook to investigate the molecular basis underlying the involvement of circ_0061825 in BC malignant progression, and this study had led to the identification of circ_0061825 knockdown that impeded BC tumorigenesis through targeting the miR-593-3p/fibroblast growth factor receptor 3 (FGFR3) axis.

Materials and Methods

Clinical Specimens and Cells

A group of 30 patients with early first primary BC, treated at Affiliated Zhongshan Hospital of Dalian University, were recruited in the present project. Primary cancer tissues and matched adjacent noncancerous tissues were

stored at -196°C in a liquid nitrogen freezer. All participants signed informed consent before the scheduled surgery, and the use of human samples was approved by the Ethics Committee of Affiliated Zhongshan Hospital of Dalian University.

Human MCF-7 and MDA-MB-231 BC cells and the immortalized MCF-10A breast epithelial cell line were provided by the American Type Culture Collection (ATCC, Manassas, VA, USA). MCF-7 cells were maintained in RPMI-1640 medium (Gibco, Bleiswijk, the Netherlands) and MDA-MB-231 were cultivated in L-15 medium (Gibco), supplemented with 10% fetal bovine serum (PAA Laboratories, Pasching, Australian) and 1% penicillin-streptomycin at 37°C with 5% CO_2 . MCF-10A cells were cultured in Dulbecco's modified Eagle's medium/Nutrient Mixture F-12 (Gibco) using standard protocols as previously reported.¹⁶

Lentivirus Transduction and Transient Transfection of Cells

For circ_0061825 knockdown in vitro studies, MCF-7 and MDA-MB-231 cells of 60% confluence were transiently transfected with 50 nM of siRNAs targeting circ_0061825 (si-circ_0061825-1, si-circ_0061825-2, si-circ_0061825-3, Ribobio, Guangzhou, China) or nontarget siRNA (si-NC) using the Lipofectamine 3000 (Invitrogen, Uppsala, Sweden). To produce FGFR3 up-regulation cells, the recombinant pcDNA-based overexpression plasmid (pc-FGFR3, 100 ng, Ribobio) was introduced into cells using Lipofectamine 3000, and the nontarget pcDNA plasmid (pc-NC) was used as the negative control. Synthetic miR-593-3p mimic and inhibitor (50 nM, Ribobio) were individually transfected into cells to generate miR-593-3p knockdown and overexpressing cells, with the scrambled oligonucleotide sequences (miRNA NC and inhibitor NC) as the control groups. For circ_0061825 knockdown in vivo assays, lentiviruses encoding short hairpin RNA (shRNA) targeting circ_0061825 (sh-circ_0061825) or nontarget shRNA (sh-NC) were used to infect MDA-MB-231 cells with various multiplicities of infection in media containing 8 $\mu\text{g}/\text{mL}$ of polybrene as recommended by the manufacturers (VectorBuilder, Guangzhou, Guangdong). Twenty-four hours after infection, the cells were placed in media in the presence of 2.5 $\mu\text{g}/\text{mL}$ of puromycin for selection over 72 h.

RNA Extraction and Quantitative Real-Time Polymerase Chain Reaction (qRT-PCR)

For total RNA preparation, clinical specimens and cells were sorted into TRIzol (Invitrogen) as per the manufacturers' guidance. Measurement of circ_0061825 and mRNA levels was conducted by TaqMan Gene Expression Assays (Applied Biosystems, Darmstadt, Germany) after cDNA synthesis using M-MLV reverse transcriptase (Invitrogen). Quantification of miR-593-3p using TaqMan MicroRNA Assay (Applied Biosystems) was done as reported¹⁷ in triplicate. Results were analyzed using the $2^{-\Delta\Delta C_t}$ method¹⁷ and normalized by the value of glyceraldehyde-3-phosphate dehydrogenase (GAPDH) or U6 expression. The primers for circ_0061825, TFF1 mRNA and miR-593-3p were synthesized by Genewiz (Suzhou, China) and their sequences were provided in Table 1.

Ribonuclease (RNase) R and Actinomycin D Assays

In RNase R assays, total cellular RNA (2.5 μ g) was incubated with 10 U of RNase R (GeneSeed, Guangzhou, China) for 30 min at 37°C, followed by the assessment of circ_0061825 and GAPDH levels by qRT-PCR.

In actinomycin D assays, MCF-7 and MDA-MB-231 cells of 70% confluence were incubated with actinomycin D (R&D Systems, Shanghai, China) at a final concentration of 2 mg/mL for 6, 12, 18 and 24 h.

Table 1 Primers Sequences Used for PCR

Primers for PCR (5'-3')		
circ_0061825	Forward	CGGCTCACAACACAGATTGA
	Reverse	GCGCAGATCACCTTGTTCTC
FGFR3	Forward	GGGACCCAGTGCAGAATGTAA
	Reverse	CAGCTTTGGGTGTGGGAGG
TFF1 linear mRNA	Forward	TTGTGGTTTTCTGGTGTCA
	Reverse	GCAGATCCCTGCAGAAGTGT
GAPDH	Forward	ATCATCAGCAATGCCTCCTG
	Reverse	ATGGACTGTGGTCATGAGTC
miR-593-3p	Forward	TGTCTCTGCTGGGTTTCT
	Reverse	GTGCAGGGTCCGAGGTATT
U6	Forward	CTCGCTTCGGCAGCAC
	Reverse	AACGCTTCACGAATTTGCGT

Abbreviations: FGFR3, fibroblast growth factor receptor 3; GAPDH, glyceraldehyde-3-phosphate dehydrogenase; PCR, polymerase chain reaction; TFF1, trefoil factor 1.

Subcellular Fractionation

Cytoplasmic and nuclear RNA were isolated from MCF-7 and MDA-MB-231 cells using the Norgen Cytoplasmic & Nuclear RNA Purification Kit as recommended by the manufacturers (Norgen Biotek, Thorold, ON, Canada). RNA (1 ng) was used for each measurement of individual circ_0061825, GAPDH and U6 levels by qRT-PCR.

Cell Viability and Colony Formation Assays

Cells were transfected with the indicated oligonucleotide or plasmid as described above, followed by the incubation for 24 h at 37°C. The Cell Counting Kit-8 (CCK-8), a sensitive colorimetric assay, was used to determine cell viability as per the suggestion of manufacturers (Abcam, Cambridge, UK). For colony formation experiments, the transfected cells were incubated for 15 days at 37°C under 5% CO₂, and then the colonies (at least 50 cells) were scored after being visualized by staining with 1% crystal violet.

Wound-Healing and Transwell Assays

A wound-healing assay for cell migration was carried out using standard protocols.¹⁸ Briefly, the cell-free gaps were created by sterile inserts at time zero (0 h). After 24 h of culture, images were acquired, and data were analyzed under an inverted microscope (Leica, Wetzlar, Germany) at 4 \times magnification. The migratory rate of wound was calculated as follows: migratory rate = $(A_0 - A_{24}) / (B_0 - B_{24})$, where A_0 represented the wound width of transfected cells at 0 h, A_{24} represented the wound width of transfected cells at 24 h, B_0 represented the wound width of untransfected cells at 0 h, B_{24} represented the wound width of untransfected cells at 24 h. Cell migration and invasion assays were performed with transwell chamber and Matrigel Invasion Chamber (8- μ m pore size, Millipore, Watford, UK), respectively. Briefly, transfected cells in FBS-free media were placed in the upper chamber of the insert, and the media containing 15% FBS was used as a chemoattractant in the lower chamber. 24 h later, the invaded or migrated cells were detected under the microscope at 100 \times magnification by being stained with crystal violet.

Flow Cytometry for Cell Cycle and Apoptosis

A Cell Cycle Kit (Dojindo, Shanghai, China) was used for the detection of cell cycle progression, according to the

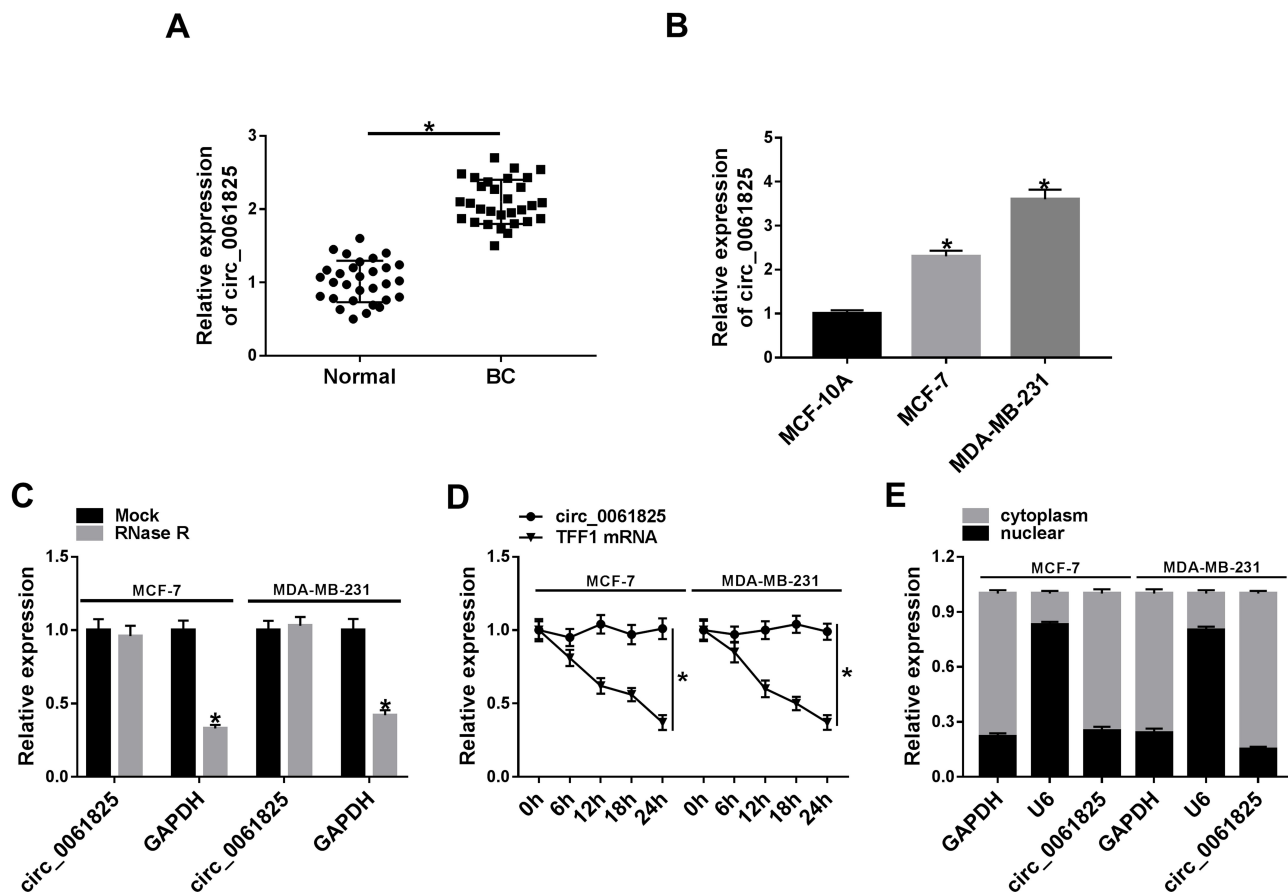


Figure 1 Circ_0061825 was overexpressed in BC tissues and cells. Circ_0061825 expression by qRT-PCR in 30 pairs of BC tissues and matched normal tissues (A), MCF-10A, MCF-7 and MDA-MB-231 cells (B). (C) Circ_0061825 and GAPDH levels by qRT-PCR in total cellular RNA incubated with RNase R. (D) The levels of circ_0061825 and TFF1 linear mRNA by qRT-PCR in MCF-7 and MDA-MB-231 cells incubated with actinomycin D. (E) Circ_0061825 expression by qRT-PCR in the cytoplasmic and nuclear fraction of MCF-7 and MDA-MB-231 cells. * $P < 0.05$.

recommendation of manufacturers. The double-staining method for cell apoptosis was performed using fluorescein isothiocyanate (FITC) labeled Annexin and propidium iodide (PI) as suggested by the manufacturers (Invitrogen). A total of ~10,000 events were used for data analysis using a flow cytometer (BD Biosciences, San Jose, CA, USA).

Bioinformatics and Dual-Luciferase Reporter Assay

Bioinformatic analyses for the targeted miRNAs of circ_0061825 and the molecular targets of miR-593-3p were carried out using CircInteractome online web (<https://circinteractome.nia.nih.gov/index.html>) and TargetScan v.7 software (http://www.targetscan.org/vert_71/). The luciferase reporter constructs harboring circ_0061825 fragment that is complementary to miR-593-3p (circ_0061825 WT) or the 3'UTR of FGFR3

mRNA (FGFR3-3'UTR WT) were provided by Cobioer (Nanjing, China). The mutations (circ_0061825 MUT and FGFR3-3'UTR MUT) in the seed region were produced by TaKaRa Mutagenesis Kit (TaKaRa, Dalian, China) based on the instructions of manufacturers using primers 5'-TGGCCGAGGCCAGAGUCUCUGGTGTACAGTG-3' (circ_0061825 MUT forward), 5'-ACCCTGGCCGAGGCCAGAGUCUCUGGTGTACA-3' (circ_0061825 MUT reverse), 5'-TGAGACTCAGTGCAGATGGUCUCUGAGCTACACAG-3' (FGFR3-3'UTR MUT forward) and 5'-CATGAGACTCAGTGCAGATGGUCUCUGAGCTACA-3' (FGFR3-3'UTR MUT reverse). Cells (5×10^4) were cotransfected with each reporter construct (100 ng) and 50 nM of miRNA NC, miR-593-3p mimic, inhibitor NC or miR-593-3p inhibitor. The ratio of firefly to Renilla luciferase activity was tested using a Dual-luciferase Assay (Promega, Leiden, The Netherlands) 36 h post-transfection.

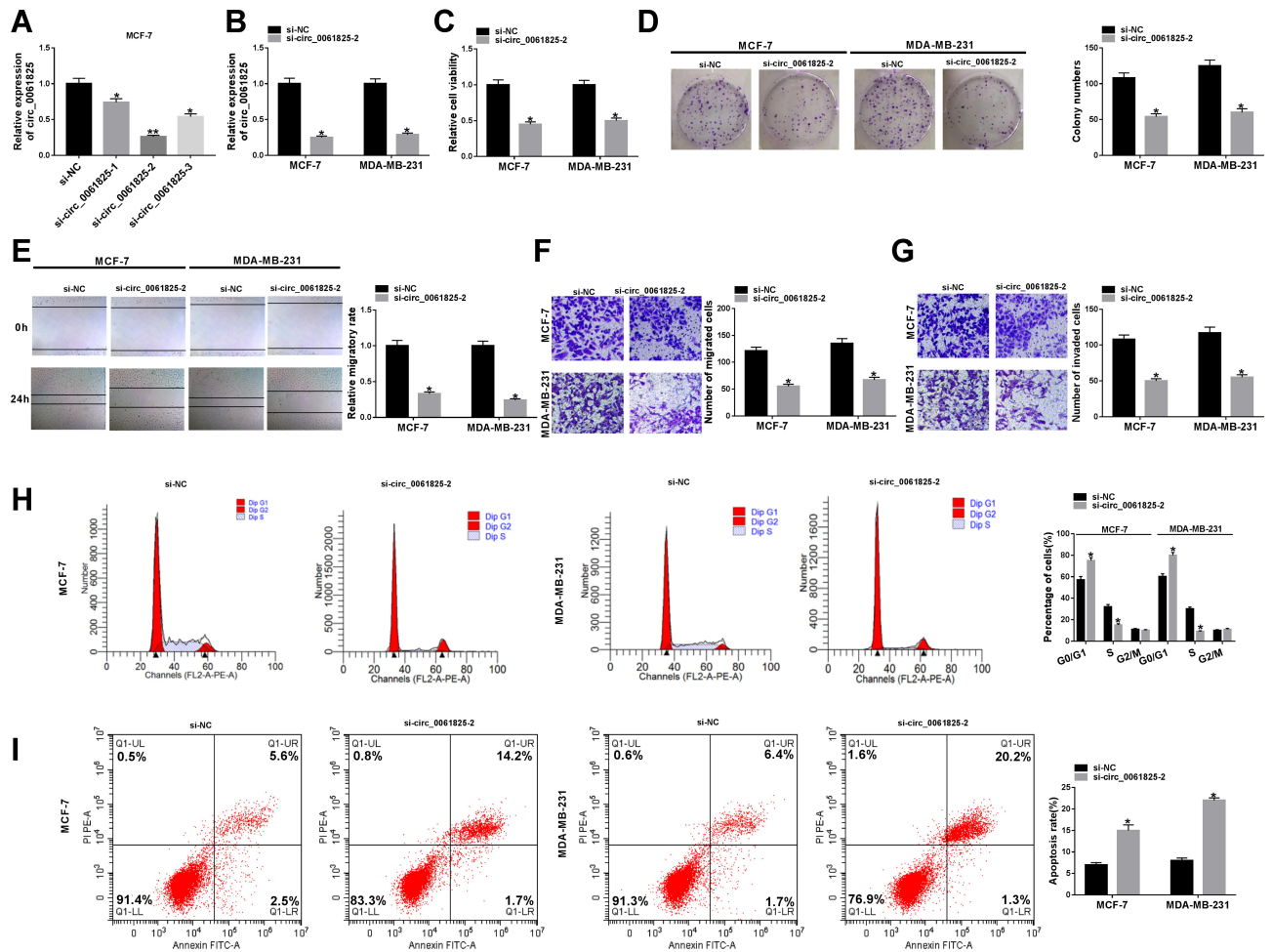


Figure 2 Circ_0061825 knockdown hindered BC cell malignant behaviors and enhanced apoptosis in vitro. (A) Circ_0061825 expression by qRT-PCR in MCF-7 cells transfected with si-NC, si-circ_0061825-1, si-circ_0061825-2 or si-circ_0061825-3. MCF-7 and MDA-MB-231 cells were transfected with si-NC or si-circ_0061825-2, followed by the measurement of circ_0061825 expression by qRT-PCR (B), cell viability by CCK-8 assay (C), colony formation using a standard colony formation assay (D), cell migration by wound-healing and transwell assays (E and F), cell invasion by transwell assay (G), cell cycle progression (H) and cell apoptosis (I) by flow cytometry. * $p < 0.05$ or ** $p < 0.01$.

Western Blot for FGFR3 Expression

Western blot was carried out using standard methods as previously reported,⁹ using antibody against FGFR3 (ab231442, Abcam) or GAPDH (ab181603, Abcam). Protein was fractionated by SDS polyacrylamide gel electrophoresis and blotted on polyvinylidene difluoride (PVDF) membranes (Millipore). The membranes were probed with the above primary antibody and horseradish peroxidase-linked IgG secondary antibody (ab97051). Blots were developed by exposure to X-ray films using the chemiluminescence system (Millipore).

Animal Studies

All animal procedures were carried out under the approval of the Ethics Committee of Affiliated Zhongshan Hospital of

Dalian University, and the guidelines set by the Academia Sinica IACUC were followed for the welfare of all animals. Male BALB/c nude mice (6-week-old, $n = 12$, ALF Biotechnology, Nanjing, China) were used in the in vivo assays. The nude mice were subcutaneously implanted with 5×10^6 sh-circ_0061825-transduced or sh-NC-infected MDA-MB-231 cells ($n = 6$ per group), and the tumors were allowed to develop for 28 days. Starting from day 7, tumor volume was detected every week. In the end, all mice were euthanized, and tumor tissues were collected.

Statistical Analysis

Groups were compared for quantitative variables using a Student's *t*-test (two-tails) or analysis of variance (ANOVA) followed by Tukey's post hoc test. Data were shown as mean \pm standard deviation (SD), and error bars

Table 2 The Putative Targeted miRNAs of Circ_0061825

Mirbase ID	Site Type	CircRNA Start	CircRNA End
hsa-miR-1231	7mer-m8	118	124
hsa-miR-326	7mer-m8	357	363
hsa-miR-593-3p	7mer-m8	123	129
hsa-miR-885-3p	7mer-1a	368	374
hsa-miR-938	7mer-m8	199	205
hsa-miR-136	7mer-1a	50	56
hsa-miR-889	8mer-1a	485	492
hsa-miR-767-3p	7mer-1a	25	31
hsa-miR-651	7mer-m8	249	255
hsa-miR-1295	7mer-1a	463	469
hsa-miR-187	7mer-m8	392	398
hsa-miR-338-3p	7mer-m8	89	95
hsa-miR-377	7mer-1a	283	289

depicted SD. Data were defined statistically significant as *P* less than 0.05.

Results

Circ_0061825 Was Overexpressed in BC Tissues and Cells

Firstly, we examined the expression of circ_0061825 in BC tissues and cell lines. As shown by qRT-PCR, in comparison to their counterparts, circ_0061825 was prominently overexpressed in BC tissues and cells (Figure 1A and B). To determine the stability of circ_0061825, we then performed RNase R and actinomycin D assays. These data revealed that GAPDH transcript was significantly decreased by RNase R digestion, and circ_0061825 was resistant to RNase R (Figure 1C). Moreover, the incubation of the BC cells with actinomycin D resulted in a remarkable down-regulation in TFF1 linear mRNA, while circ_0061825 level did not reduce in the assayed time frame (Figure 1D). Additionally, the data of subcellular localization revealed that circ_0061825 was mainly localized in the cytoplasm of MCF-7 and MDA-MB-231 cells (Figure 1E).

Circ_0061825 Knockdown Restrained BC Cell Viability, Colony Formation, Migration, Invasion, Cell Cycle Progression and Accelerated Cell Apoptosis in vitro

To evaluate the functional effect of circ_0061825 on BC tumorigenesis, we performed loss-of-function

analyses with siRNA-circ_0061825 (si-circ_0061825) in MCF-7 and MDA-MB-231 cells. The transfection of si-circ_0061825, but not the negative control si-NC, induced a significant reduction in circ_0061825 expression in MCF-7 cells (Figure 2A). Remarkably, si-circ_0061825-2 induced a more distinct down-regulation in circ_0061825, so we selected it for further research. By contrast, circ_0061825 expression was strikingly decreased in si-circ_0061825-2-transfected MDA-MB-231 cells (Figure 2B). Additionally, no reduction was observed in TFF1 linear mRNA level in the presence of si-circ_0061825-2 (Supplement Figure 1). Functional analyses revealed that in contrast to the negative control, circ_0061825 knockdown led to a prominent suppression in cell viability (Figure 2C), colony formation (Figure 2D), migration (Figure 2E and F), invasion (Figure 2G) and cell cycle progression (Figure 2H), as well as a striking enhancement in cell apoptosis (Figure 2I) in the two BC cells.

Circ_0061825 Acted as a Molecular Sponge of miR-593-3p

We then determined the molecular basis by which circ_0061825 regulated BC cell malignant progression. Using CircInteractome online tool, the predicted data showed that there are 13 putative candidate miRNAs that bind to circ_0061825 (Table 2). We then detected the impact of circ_0061825 on several BC-related miRNAs, and we found that miR-593-3p was the most significantly up-regulated miRNA as a result of circ_0061825 silencing in MCF-7 cells (Supplement Figure 2). Thus, we selected miR-593-3p for further analysis. To validate the validity of the target region for interaction between circ_0061825 and miR-593-3p, we cloned circ_0061825 fragment harboring the miR-593-3p-binding region into a luciferase vector and mutated the seed region (Figure 3A). The data of qRT-PCR showed that the introduction of miR-593-3p mimic significantly elevated miR-593-3p expression in the two BC cells (Figure 3B). With circ_0061825 luciferase reporter construct (WT-circ_0061825) and miR-593-3p overexpression led to a striking down-regulation in luciferase activity, but the mutation of the seed sequence (MUT-circ_0061825) notably abolished the reduced effect of miR-593-3p overexpression (Figure 3C). The transfection efficiency of miR-593-3p inhibitor was gauged by qRT-PCR (Figure 3D).

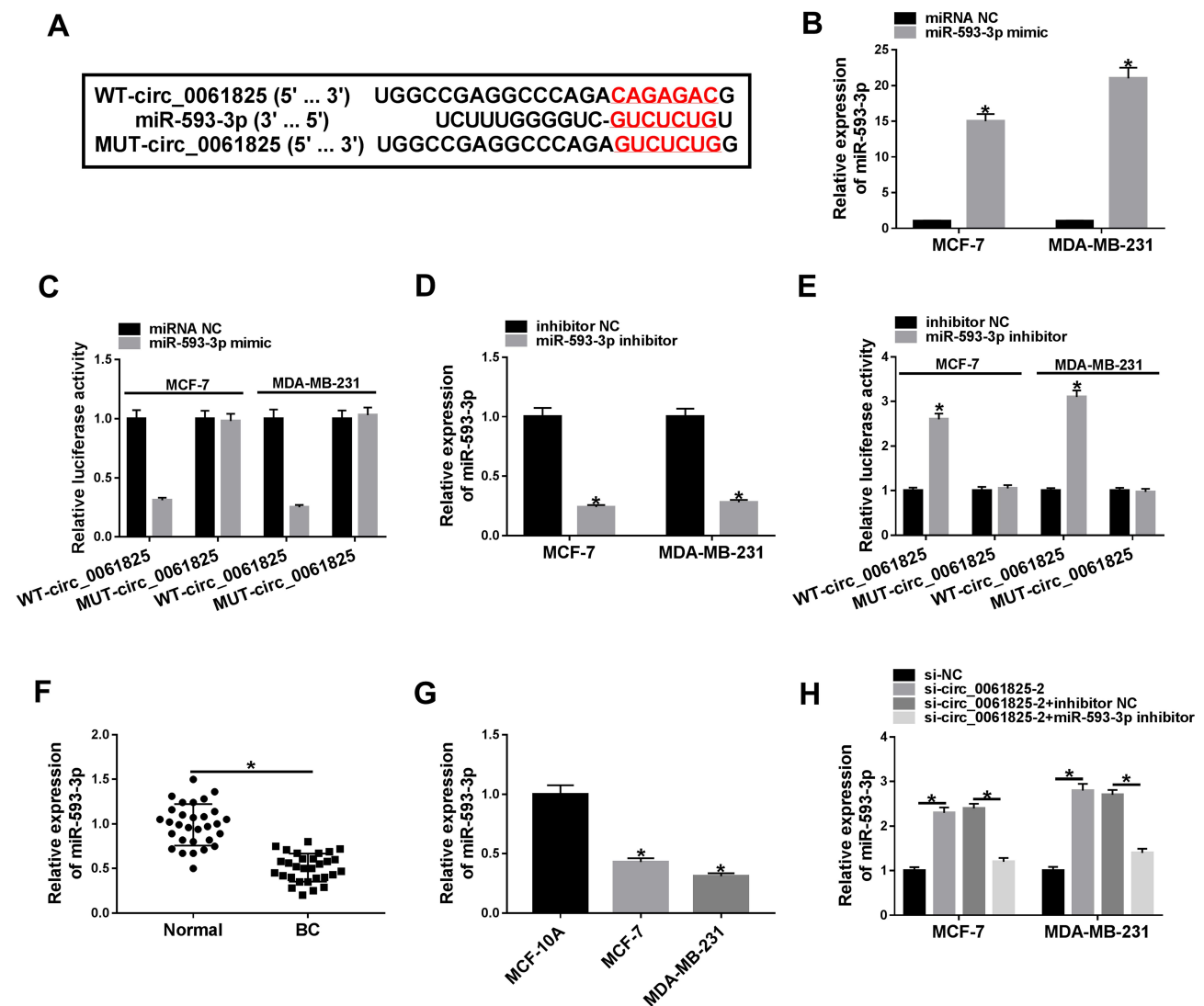


Figure 3 Circ_0061825 acted as a molecular sponge of miR-593-3p. (A) Schematic of the predicted complementary sequence for miR-593-3p in circ_0061825 and the mutation of the seed sequence. (B) MiR-593-3p expression by qRT-PCR in MCF-7 and MDA-MB-231 cells transfected with miRNA NC or miR-593-3p mimic. (C) Dual-luciferase reporter assays in the two BC cells. (D) MiR-593-3p expression in MCF-7 and MDA-MB-231 cells transfected with inhibitor NC or miR-593-3p inhibitor. (E) Dual-luciferase reporter assays in the two BC cells. MiR-593-3p expression by qRT-PCR in 30 pairs of BC tissues and matched normal tissues (F), MCF-10A, MCF-7 and MDA-MB-231 cells (G), MCF-7 and MDA-MB-231 cells transfected with si-NC, si-circ_0061825-2, si-circ_0061825-2+inhibitor NC or si-circ_0061825-2+miR-593-3p inhibitor (H). * $P < 0.05$.

Transient transfection of WT-circ_0061825 in the presence of miR-593-3p inhibitor caused a prominent elevation of relative luciferase activity, and this effect was completely abrogated by MUT-circ_0061825 (Figure 3E). The results of qRT-PCR also showed that miR-593-3p was significantly underexpressed in BC tissues and cells (Figure 3F and G). Furthermore, in comparison to their counterparts, miR-593-3p expression was notably increased by circ_0061825 knockdown in the two cells, while this effect was significantly reversed when the transfection of miR-593-3p inhibitor (Figure 3H).

Circ_0061825 Knockdown Regulated BC Cell Viability, Colony Formation, Migration, Invasion, Cell Cycle Progression and Apoptosis in vitro by miR-593-3p

Next, we asked whether circ_0061825 regulated BC cell malignant progression by miR-593-3p. As expected, in comparison the control group, circ_0061825 knockdown-induced anti-viability (Figure 4A), anti-colony formation (Figure 4B), anti-migration, anti-invasion (Figure 4C and D), cell cycle arrest (Figure 4E) and pro-apoptosis (Figure

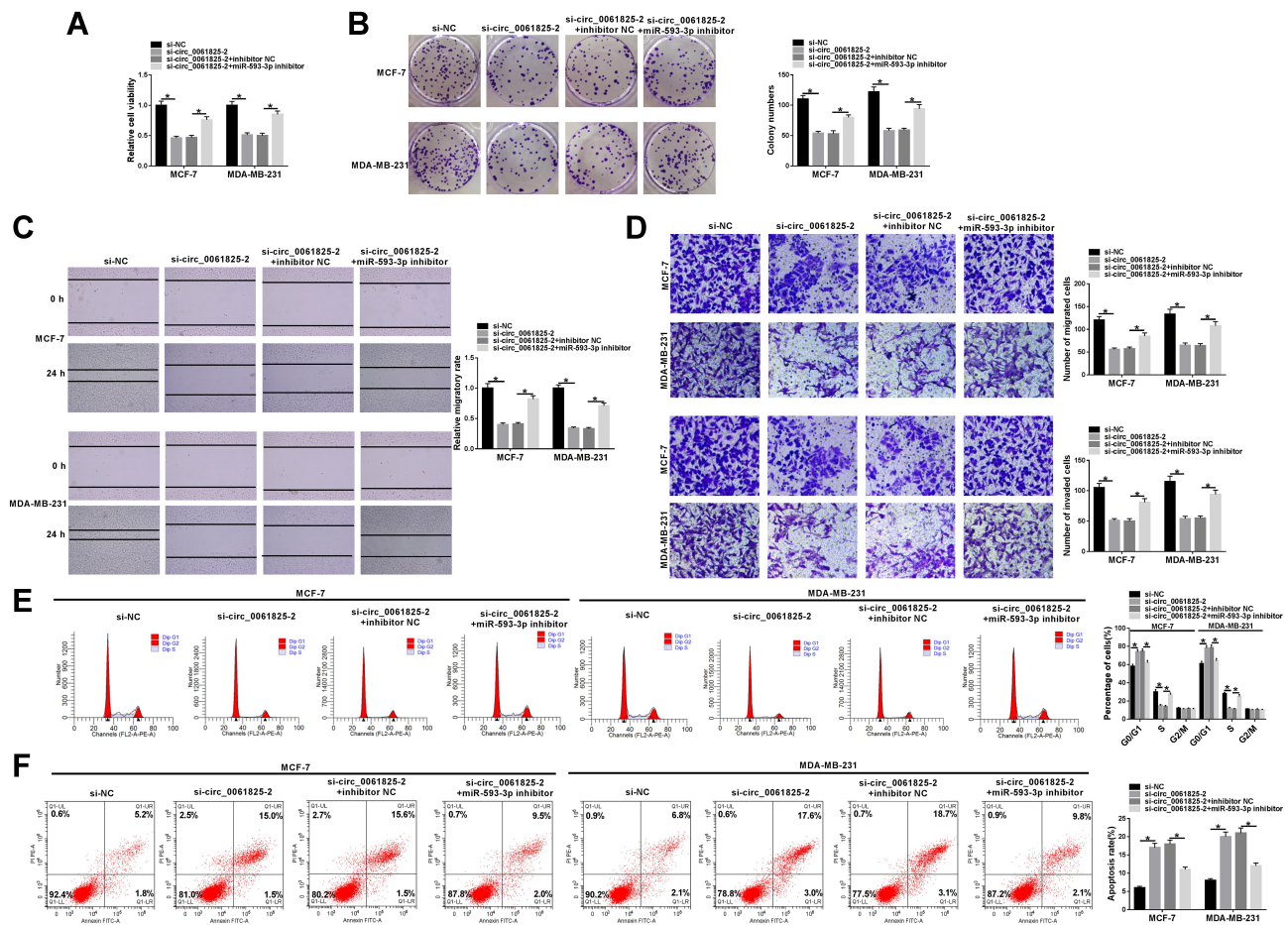


Figure 4 The knockdown of circ_0061825 repressed BC cell malignant progression in vitro by miR-593-3p. MCF-7 and MDA-MB-231 cells were transfected with si-NC, si-circ_0061825-2, si-circ_0061825-2+inhibitor NC or si-circ_0061825-2+miR-593-3p inhibitor. (A) CCK-8 assay for cell viability. (B) A standard colony formation assay for cell colony formation. (C) Wound-healing assay for cell migration. (D) Transwell assay for cell migration and invasion. (E and F) Flow cytometry for cell cycle progression and apoptosis. * $P < 0.05$.

4F) effects were prominently reversed by the transfection of miR-593-3p inhibitor.

MiR-593-3p Directly Interacted with the 3'UTR of FGFR3

To further understand the role of miR-593-3p in BC malignant progression, we used computational methods to help identify its molecular targets. Among these candidates, we detected the impact of miR-593-3p on several BC-related genes expression in BC cells, and we found that the reduced level of miR-593-3p led to the most significant up-regulation of FGFR3 mRNA level in MCF-7 cells (Supplement Figure 3). So, we selected FGFR3 for further investigation in this study. To confirm whether FGFR3 was a target of miR-593-

3p, we cloned the 3'UTR of FGFR3 into a luciferase plasmid and mutated the target sequence (Figure 5A). When we performed dual-luciferase reporter assays, the cotransfection of FGFR3 3'UTR luciferase reporter (WT-FGFR3-3'UTR) and miR-593-3p mimic into the two BC cells generated lower luciferase activity than in cells cotransfected with miRNA NC control (Figure 5B), while the cotransfection of miR-593-3p inhibitor produced higher luciferase activity than in the control group (Figure 5C). However, the regulatory impact of miR-593-3p on reporter gene expression was strongly abrogated by the FGFR3 3'UTR mutation (MUT-FGFR3-3'UTR, Figure 5B and C). The data of Western blot revealed a significant up-regulation of FGFR3 expression in BC tissues and cells (Figure 5D and E).

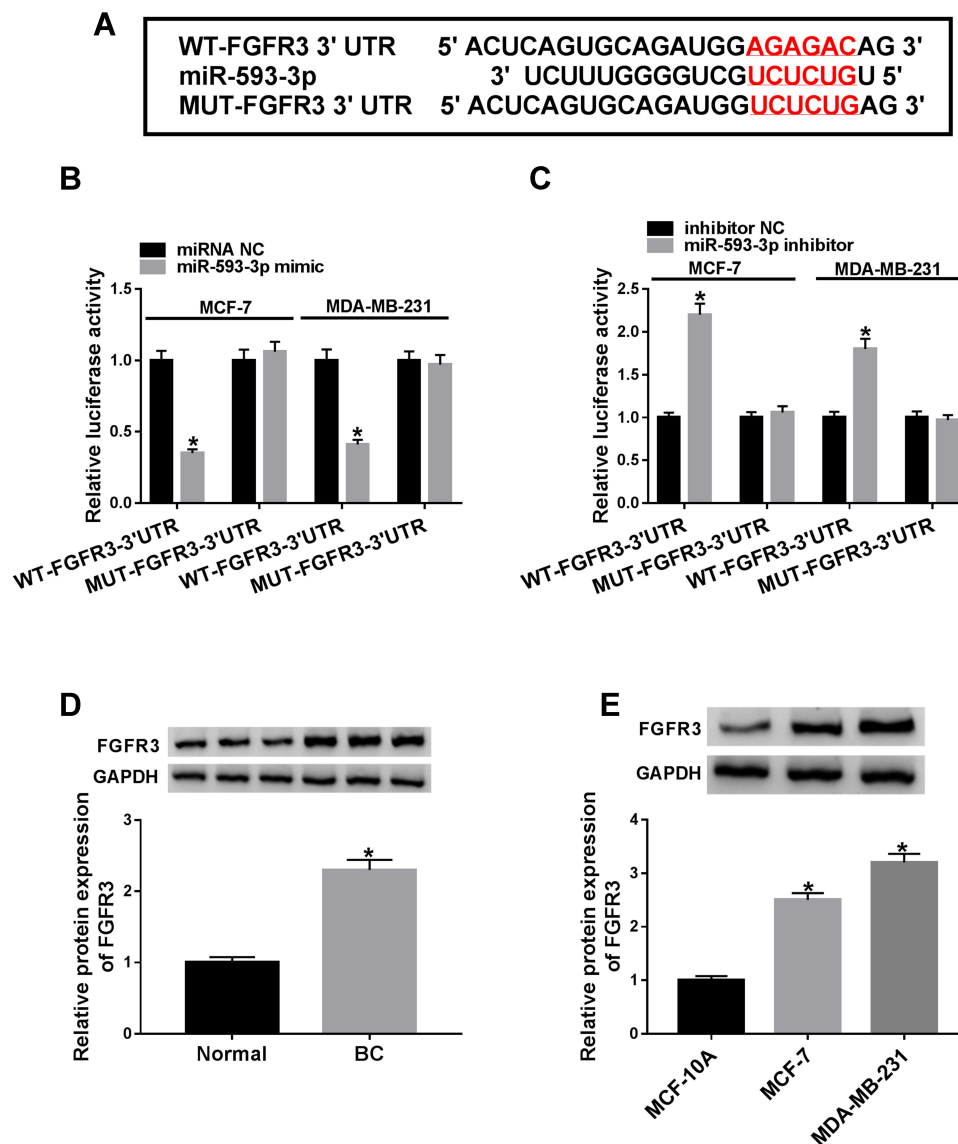


Figure 5 MiR-593-3p directly interacted with the 3'UTR of FGFR3. (A) Schematic model of the putative miR-593-3p binding sequence in the 3'UTR of FGFR3 mRNA and mutated the miR-593-3p-binding sequence. (B and C) Dual-luciferase reporter assay in MCF-7 and MDA-MB-231 cells. FGFR3 protein expression by Western blot in 3 pairs of BC tissues and matched normal tissues (D), MCF-10A, MCF-7 and MDA-MB-231 cells (E). * $P < 0.05$.

FGFR3 Was a Functional Target of miR-593-3p in Regulating BC Cell Viability, Colony Formation, Migration, Invasion, Cell Cycle Progression and Apoptosis in vitro

To provide further mechanistic insight into the link between miR-593-3p and FGFR3 in BC malignant progression, the two BC cells were transfected with miR-593-3p mimic alone or together with FGFR3 over-expression plasmid (pc-FGFR3). Transient transfection of pc-FGFR3, but not the negative plasmid pc-NC, significantly elevated the expression of FGFR3 in the

two cells (Figure 6A). Western blot analyses also revealed that the elevated level of miR-593-3p triggered a striking reduction in FGFR3 expression (Figure 6B). Functional experiments results showed that in contrast to the control group, the elevated level of miR-593-3p resulted in a remarkable suppression in cell viability (Figure 6C), colony formation (Figure 6D), migration, invasion (Figure 6E and F) and cell cycle progression (Figure 6G), as well as a striking promotion in cell apoptosis (Figure 6H). Nevertheless, these effects of the elevated miR-593-3p level were significantly reversed by pc-FGFR3 cotransfection in the two BC cells (Figure 6B–H).

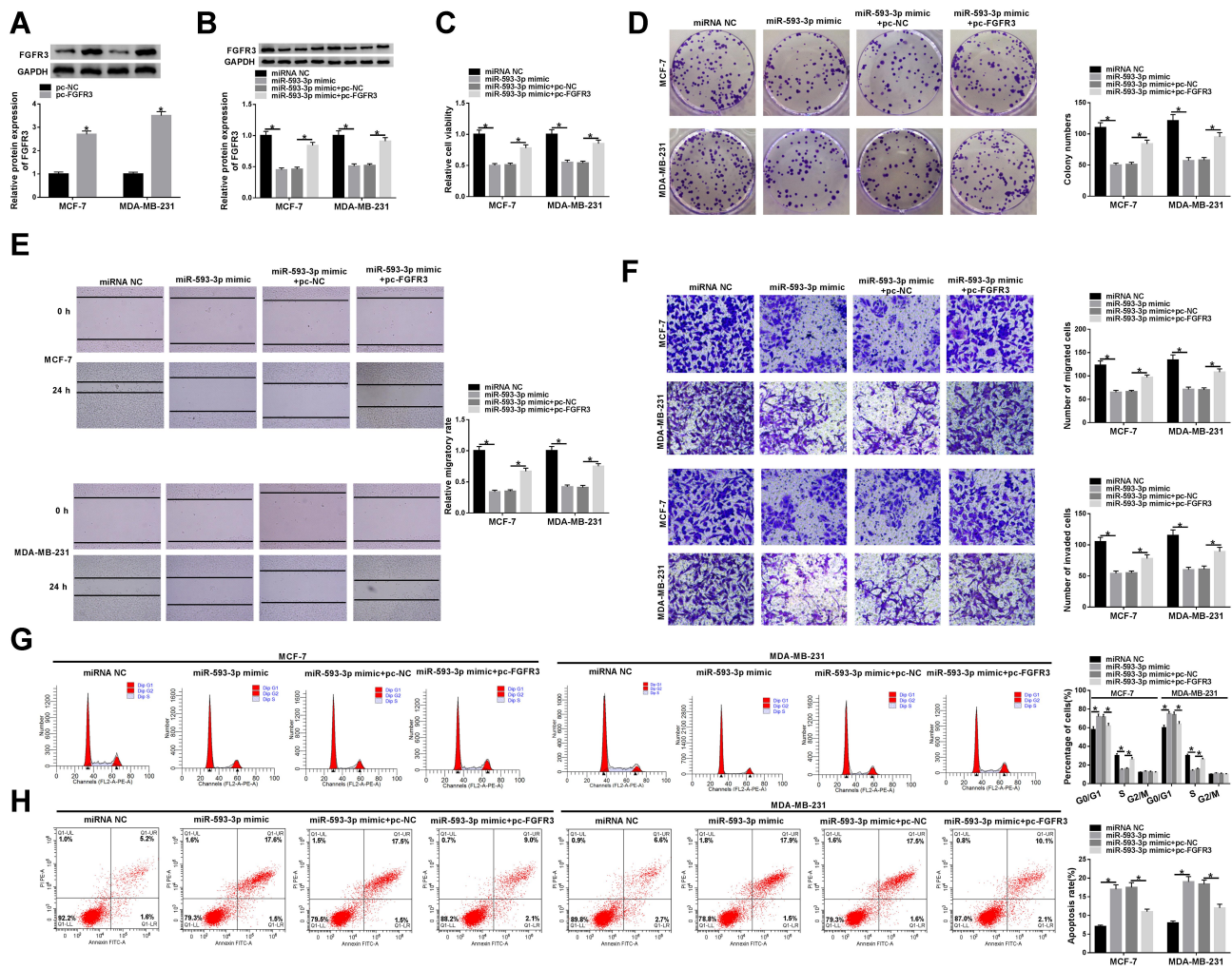


Figure 6 Mir-593-3p overexpression hindered BC cell malignant progression in vitro by FGFR3. (A) FGFR3 expression by Western blot in MCF-7 and MDA-MB-231 cells transfected with pc-NC or pc-FGFR3. MCF-7 and MDA-MB-231 cells were transfected with miRNA NC, miR-593-3p mimic, miR-593-3p mimic+pc-NC, miR-593-3p mimic+pc-FGFR3, followed by the detection of FGFR3 expression by Western blot (B), cell viability (C), cell colony formation using a standard colony formation assay (D), cell migration and invasion by wound-healing or transwell assay (E and F), cell cycle progression (G) and apoptosis (H) by flow cytometry. *P < 0.05.

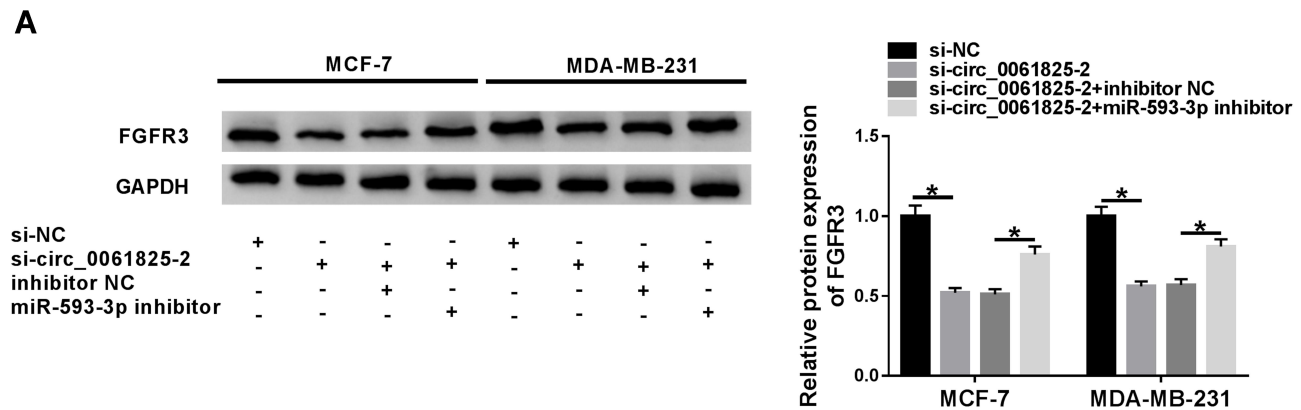


Figure 7 Circ_0061825 modulated FGFR3 expression through sponging miR-593-3p. (A) FGFR3 protein expression by Western blot in MCF-7 and MDA-MB-231 cells transfected with si-NC, si-circ_0061825-2, si-circ_0061825-2+inhibitor NC or si-circ_0061825-2+miR-593-3p inhibitor. *P < 0.05.

Circ_0061825 Influenced FGFR3 Expression by Acting as a Sponge of miR-593-3p

We also determined whether circ_0061825 regulated FGFR3 expression through acting as a miRNA sponge. In comparison to the corresponding control group, FGFR3 protein expression was dramatically down-regulated by circ_0061825 knockdown in the two BC cells, and this effect was prominently abrogated by the transfection of miR-593-3p inhibitor (Figure 7A).

Circ_0061825 Knockdown Hampered Tumor Growth in vivo

Lastly, we undertook to evaluate whether circ_0061825 could influence tumor growth in vivo. To address this, we established the xenograft models using sh-circ_0061825-transduced or sh-NC-infected MDA-MB-231 cells by subcutaneous implantation. In contrast to the sh-NC group, the transduction of sh-circ_0061825 led to a significant repression in tumor growth (Figure 8A and B). Moreover, circ_0061825 and FGFR3 were down-regulated and miR-593-3p was up-regulated in tumor

tissues derived from sh-circ_0061825-transduced cells (Figure 8C–E).

Discussion

Until now, hundreds of circRNAs have been identified, many of them expressed in tumor tissues and linked to human carcinogenesis, including BC.^{19,20} Of these circRNAs, circ_0061825 was a strong candidate in BC pathogenesis, considering its oncogenic property for BC tumorigenesis.¹⁰ In the current report, we aimed to explore precise action of circ_0061825 in BC malignant progression, with the hope that this investigation might provide a novel mechanism of circRNAs in BC pathogenesis.

Here, we validated a significant overexpression of circ_0061825 in BC, consistent with the findings by Pan et al.¹⁰ As has previously been reported for other circRNAs,^{21,22} circ_0061825 were resistant to RNase R and its level did not decrease when incubation with actinomycin D, demonstrating the inherent stability of circ_0061825, which is attributed to their loop structures without 5' and 3' ends.²³ Our data also identified the repressive function of circ_0061825 knockdown on BC cell malignant behaviors in vitro and tumor growth in vivo.

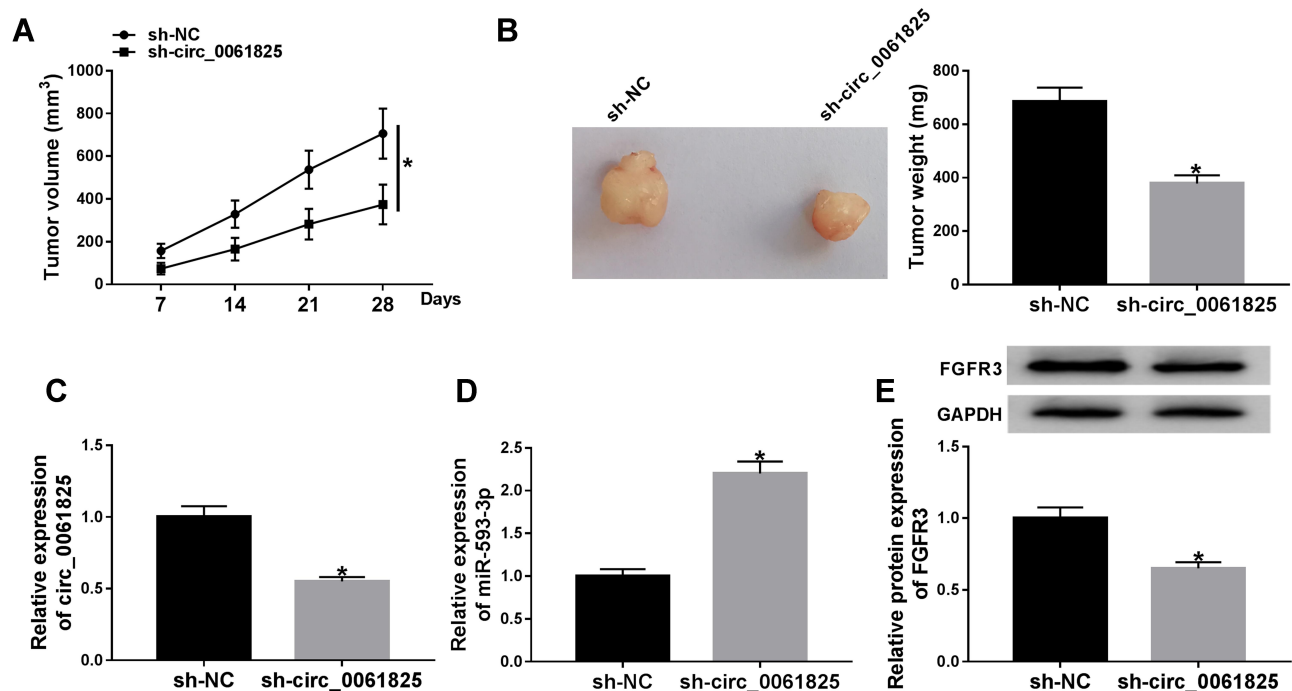


Figure 8 Circ_0061825 knockdown mitigated tumor growth in vivo. sh-circ_0061825-transduced or sh-NC-infected MDA-MB-231 cells were subcutaneously implanted into the nude mice (n = 6 per group). 28 days later, all mice were euthanized, and tumor tissues were removed. (A) After 7 days of implantation, tumor volume measurement began and was performed every week. (B) Tumor average weight was calculated and representative pictures were photographed. Circ_0061825 expression (C) and miR-593-3p level (D) by qRT-PCR, and FGFR3 expression by Western blot (E) in the xenograft tissues. **P* < 0.05.

Additionally, we showed the cytoplasmic localization of circ_0061825 in BC cells, offering the possibility for the function of circ_0061825 as miRNA sponges.²⁴

Using the CircInteractome database,²⁵ we first demonstrated that circ_0061825 directly targeted miR-593-3p. Among these candidates, miR-593-3p was interesting in the current report owing to its important involvement in human cancers, such as nasopharyngeal carcinoma, gastric cancer and non-small cell lung cancer.^{13,26,27} Here, we uncovered that miR-593-3p overexpression performed an inhibitory effect on BC cell malignant progression in vitro. For the first time, our data showed that circ_0061825 knockdown weakened BC malignant progression in vitro by up-regulating miR-539-3p.

The mutation and overexpression of FGFR3 have been reported to be closely associated with an unfavourable prognosis of certain human cancers, such as tongue cancer, colorectal cancer and papillary bladder cancer.^{28–30} The gene fusions of FGFR3-transforming acidic coiled-coil containing protein 3 (TACC3) in cancer are indicated as one of the most recurrent fusions in almost all types of tumors.^{31,32} Long et al uncovered that FGFR3 was overexpressed in BC and the depletion of FGFR3 exerted a repressive activity in BC cell malignant behaviors.³³ Our work was first to identify that FGFR3 was a direct target of miR-593-3p and circ_0061825 served as a sponge of miR-593-3p to mediate FGFR3 expression in BC cells. More importantly, we first demonstrated that miR-593-3p overexpression hindered BC cell malignant progression in vitro via down-regulating FGFR3. Similarly, Long and colleagues illuminated that miR-99a functioned as a tumor-suppressor in BC tumorigenesis through targeting FGFR3.³³ In vivo assays demonstrated that the miR-593-3p/FGFR3 axis was regulated by circ_0061825 in xenograft tumors. However, the direct in vivo evidence about the interplay of circ_0061825 and the miR-593-3p/FGFR3 axis on BC pathogenesis was absent, which is expected to be investigated in further work.

In conclusion, our current findings provided evidence that circ_0061825, an up-regulated circRNA in BC, regulated BC malignant progression through targeting the miR-593-3p/FGFR3 axis, highlighting a novel mechanism basis of circRNA in BC pathogenesis. A further challenge will be to identify the clinical significance of circ_0061825 and its potential value as a therapeutic target for BC management.

Abbreviations

BC, Breast cancer; circRNAs, Circular RNAs; qRT-PCR, quantitative real-time polymerase chain reaction; FGFR3, fibroblast growth factor receptor 3; RNase, ribonuclease; CCK-8, Cell Counting Kit-8; FITC, fluorescein isothiocyanate; PI, propidium iodide; ANOVA, analysis of variance.

Ethics Approval and Consent to Participate

The hospital's Institutional Review Board approved the current study.

Funding

The present study was supported by 2016 medical research fund project of Dalian health and Family Planning Commission (No.16.1.1.110).

Disclosure

The authors declare that they have no financial conflicts of interest.

References

- Bray F, Ferlay J, Soerjomataram I, Siegel RL, Torre LA, Jemal A. Global cancer statistics 2018: GLOBOCAN estimates of incidence and mortality worldwide for 36 cancers in 185 countries. *CA Cancer J Clin*. 2018;68(6):394–424. doi:10.3322/caac.21492.
- Jhan JR, Andrechek ER. Triple-negative breast cancer and the potential for targeted therapy. *Pharmacogenomics*. 2017;18(17):1595–1609. doi:10.2217/pgs-2017-0117.
- Collignon J, Lousberg L, Schroeder H, Jerusalem G. Triple-negative breast cancer: treatment challenges and solutions. *Breast Cancer (Dove Med Press)*. 2016;8:93–107. doi:10.2147/bctt.s69488.
- Jeck WR, Sharpless NE. Detecting and characterizing circular RNAs. *Nat Biotechnol*. 2014;32(5):453–461. doi:10.1038/nbt.2890.
- Kristensen LS, Hansen TB, Venø MT, Kjems J. Circular RNAs in cancer: opportunities and challenges in the field. *Oncogene*. 2018;37(5):555–565. doi:10.1038/onc.2017.361.
- Nair AA, Niu N, Tang X, et al. As and their associations with breast cancer subtypes. *Oncotarget*. 2016;7(49):80967–80979. doi:10.18632/oncotarget.13134.
- Wang H, Xiao Y, Wu L, Ma D. Comprehensive circular RNA profiling reveals the regulatory role of the circRNA-000911/miR-449a pathway in breast carcinogenesis. *Int J Oncol*. 2018;52(3):743–754. doi:10.3892/ijo.2018.4265.
- Zhang HD, Jiang LH, Hou JC, et al. Circular RNA hsa_circ_0052112 promotes cell migration and invasion by acting as sponge for miR-125a-5p in breast cancer. *Biomed Pharmacother*. 2018;107:1342–1353. doi:10.1016/j.biopha.2018.08.030.
- Liu Y, Lu C, Zhou Y, Zhang Z, Sun L. Circular RNA hsa_circ_0008039 promotes breast cancer cell proliferation and migration by regulating miR-432-5p/E2F3 axis. *Biochem Biophys Res Commun*. 2018;502(3):358–363. doi:10.1016/j.bbrc.2018.05.166.
- Pan G, Mao A, Liu J, Lu J, Ding J, Liu W. Circular RNA hsa_circ_0061825 (circ-TFF1) contributes to breast cancer progression through targeting miR-326/TFF1 signalling. *Cell Prolif*. 2020;53(2):e12720. doi:10.1111/cpr.12720.

11. Dvinge H, Git A, Gräf S, et al. The shaping and functional consequences of the microRNA landscape in breast cancer. *Nature*. 2013;497(7449):378–382. doi:10.1038/nature12108.
12. Tavazoie SF, Alarcón C, Oskarsson T, et al. Endogenous human microRNAs that suppress breast cancer metastasis. *Nature*. 2008;451(7175):147–152. doi:10.1038/nature06487.
13. Fan H, Shao M, Huang S, et al. MiR-593 mediates curcumin-induced radiosensitization of nasopharyngeal carcinoma cells via MDR1. *Oncol Lett*. 2016;11(6):3729–3734. doi:10.3892/ol.2016.4438.
14. Wei F, Wang M, Li Z, Wang Y, Zhou Y. miR-593 inhibits proliferation and invasion and promotes apoptosis in non-small cell lung cancer cells by targeting SLUG-associated signaling pathways. *Mol Med Rep*. 2019;20(6):5172–5182. doi:10.3892/mmr.2019.10776.
15. Song L, Xiao Y. Downregulation of hsa_circ_0007534 suppresses breast cancer cell proliferation and invasion by targeting miR-593/MUC19 signal pathway. *Biochem Biophys Res Commun*. 2018;503(4):2603–2610. doi:10.1016/j.bbrc.2018.08.007.
16. Daly CS, Flemban A, Shafei M, Conway ME, Qualtrough D, Dean SJ. Hypoxia modulates the stem cell population and induces EMT in the MCF-10A breast epithelial cell line. *Oncol Rep*. 2018;39(2):483–490. doi:10.3892/or.2017.6125.
17. Rivetti Di Val Cervo P, Lena AM, Nicoloso M. p63-microRNA feedback in keratinocyte senescence. *Proc Natl Acad Sci U S A*. 2012;109(4):1133–1138. doi:10.1073/pnas.1112257109.
18. Cappiello F, Casciaro B, Mangoni ML. A novel in vitro wound healing assay to evaluate cell migration. *J Vis Exp*. 2018;(133):56825. doi:10.3791/56825.
19. Smid M, Wilting SM, Uhr K, Rodríguez-González FG, de Weerd V. The circular RNome of primary breast cancer. *Genome Res*. 2019;29(3):356–366. doi:10.1101/gr.238121.118.
20. Li Z, Chen Z, Hu G, Jiang Y. Roles of circular RNA in breast cancer: present and future. *Am J Transl Res*. 2019;11(7):3945–3954.
21. Li F, Zhang L, Li W, et al. Circular RNA ITCH has inhibitory effect on ESCC by suppressing the Wnt/β-catenin pathway. *Oncotarget*. 2015;6(8):6001–6013. doi:10.18632/oncotarget.3469.
22. Wang J, Li X, Lu L, He L, Hu H, Xu Z. Circular RNA hsa_circ_0000567 can be used as a promising diagnostic biomarker for human colorectal cancer. *J Clin Lab Anal*. 2018;32(5):e22379. doi:10.1002/jcla.22379.
23. Du WW, Zhang C, Yang W, Yong T, Awan FM, Yang BB. Identifying and characterizing circRNA-protein interaction. *Theranostics*. 2017;7(17):4183–4191. doi:10.7150/thno.21299.
24. Verduci L, Strano S, Yarden Y, Blandino G. The circRNA-microRNA code: emerging implications for cancer diagnosis and treatment. *Mol Oncol*. 2019;13(4):669–680. doi:10.1002/1878-0261.12468.
25. Dudekula DB, Panda AC, Grammatikakis I, De S, Abdelmohsen K, Gorospe M. CircInteractome: a web tool for exploring circular RNAs and their interacting proteins and microRNAs. *RNA Biol*. 2016;13(1):34–42. doi:10.1080/15476286.2015.1128065.
26. Dong L, Hong H, Chen X, Huang Z, Wu W, Wu F. LINC02163 regulates growth and epithelial-to-mesenchymal transition phenotype via miR-593-3p/FOXK1 axis in gastric cancer cells. *Artif Cells Nanomed Biotechnol*. 2018;46(sup2):607–615. doi:10.1080/21691401.2018.1464462.
27. Han W, Wang L, Zhang L, Wang Y, Li Y. Circular RNA circ-RAD23B promotes cell growth and invasion by miR-593-3p/CCND2 and miR-653-5p/TIAMI pathways in non-small cell lung cancer. *Biochem Biophys Res Commun*. 2019;510(3):462–466. doi:10.1016/j.bbrc.2019.01.131.
28. Bersani C, Haegglblom L, Ursu RG, et al. Overexpression of FGFR3 in HPV-positive tonsillar and base of tongue cancer is correlated to outcome. *Anticancer Res*. 2018;38(8):4683–4690. doi:10.21873/anticancer.12774.
29. Fromme JE, Schildhaus HU. FGFR3 overexpression is a relevant alteration in colorectal cancer. *Pathologie*. 2018;39(Suppl 2):189–192. doi:10.1007/s00292-018-0504-0.
30. Geelvink M, Babmorad A, Maurer A, Stöhr R, Grimm T. Diagnostic and prognostic implications of FGFR3(high)/Ki67(high) papillary bladder cancers. *Int J Mol Sci*. 2018;19(9):2548. doi:10.3390/ijms19092548.
31. Frattini V, Pagnotta SM, Tala FJJ, et al. A metabolic function of FGFR3-TACC3 gene fusions in cancer. *Nature*. 2018;553(7687):222–227. doi:10.1038/nature25171.
32. Costa R, Carneiro BA, Taxter T, et al. FGFR3-TACC3 fusion in solid tumors: mini review. *Oncotarget*. 2016;7(34):55924–55938. doi:10.18632/oncotarget.10482.
33. Long X, Shi Y, Ye P, Guo J, Zhou Q, Tang Y. MicroRNA-99a suppresses breast cancer progression by targeting FGFR3. *Front Oncol*. 2019;9:1473. doi:10.3389/fonc.2019.01473.

Cancer Management and Research

Dovepress

Publish your work in this journal

Cancer Management and Research is an international, peer-reviewed open access journal focusing on cancer research and the optimal use of preventative and integrated treatment interventions to achieve improved outcomes, enhanced survival and quality of life for the cancer patient.

The manuscript management system is completely online and includes a very quick and fair peer-review system, which is all easy to use. Visit <http://www.dovepress.com/testimonials.php> to read real quotes from published authors.

Submit your manuscript here: <https://www.dovepress.com/cancer-management-and-research-journal>